Distributed representations of prediction error signals across the cortical hierarchy are synergistic

Frank Gelens[a,b], Misako Komatsu[c], Cem Uran[d,e], Michael A. Jensen[f], Kai J. Miller[f], Robin A.A. Ince[g], Martin Vinck[d,e,i], Andres Canales-Johnson[b,h,i]

[a]*Department of Psychology, University of Amsterdam, Nieuwe Achtergracht 129-B, 1018 WT, Amsterdam, The Netherlands*
[b]*Department of Psychology, University of Cambridge, CB2 3EB Cambridge, United Kingdom*
[c]*Laboratory for Adaptive Intelligence, RIKEN Brain Science Institute, Saitama 351-0198, Japan*
[d]*Ernst Strüngmann Institute (ESI) for Neuroscience in Cooperation with Max Planck Society, 60528 Frankfurt am Main, Germany*
[e]*Donders Centre for Neuroscience, Department of Neuroinformatics, Radboud University Nijmegen, 6525 Nijmegen, Netherlands*
[f]*Department of Neurosurgery, Mayo Clinic, Rochester, Minnesota 55905*
[g]*Institute of Neuroscience and Psychology, University of Glasgow, Scotland G12 8QB, United Kingdom*
[h]*Neuropsychology and Cognitive Neurosciences Research Center, Faculty of Health Sciences, Universidad Católica del Maule, 3460000 Talca, Chile*
[i]*Correspondence to: Andres Canales-Johnson (afc37@cam.ac.uk), Martin Vinck (martin.vinck@esi-frankfurt.de)*

Abstract

An important question concerning inter-areal communication in the cortex, is whether these interactions are synergistic, i.e. convey information beyond what can be performed by isolated signals. Here, we dissociated cortical interactions sharing common information from those encoding complementary information during prediction error processing. To this end, we computed co-information, an information-theoretical measure that distinguishes redundant from synergistic information among brain signals. We analyzed auditory and frontal electrocorticography (ECoG) signals in three common awake marmosets and investigated to what extent event-related-potentials (ERP) and broadband (BB) dynamics exhibit redundancy and synergy in auditory prediction error signals. We observed multiple patterns of redundancy and synergy across the entire cortical hierarchy with distinct dynamics. The information conveyed by ERPs and BB signals was highly synergistic even at lower stages of the hierarchy in the auditory cortex, as well as between lower and higher areas in the frontal cortex. These results indicate that the distributed representations of prediction error signals across the cortical hierarchy can be highly synergistic.

INTRODUCTION

The traditional modular view of brain function is increasingly challenged by the finding that information about external stimuli and internal variables is distributed across brain areas (de Schotten and Forkel, 2022; Urai et al., 2022; Shenoy and Kao, 2021; Breakspear, 2017; Panzeri et al., 2022). When information in a complex system is carried by multiple nodes, this could imply that there is a large degree of redundancy in the information carried by the different nodes. That is, the whole is actually less than the sum of the parts. An alternative possibility, however, is that information is carried in a synergistic manner, i.e. the different nodes might carry extra information about task variables when they are combined. In other words, the whole is more than the sum of the parts (Luppi et al., 2022).

Both recent large-scale spiking and electrocorticographic (ECoG) recordings support the notion that information about task variables is widely distributed rather than highly localized (Urai et al., 2022; Steinmetz et al., 2019; Parras et al., 2017; Saleem et al., 2018; Voitov and Mrsic-Flogel, 2022). For example, in the visual domain, widespread neuronal patterns across nearly every brain region are non-selectively activated before movement onset during a visual choice task (Steinmetz et al., 2019). Similarly, distributed and reciprocally interconnected areas of the cortex maintain high-dimensional representations of working memory (Voitov and Mrsic-Flogel, 2022). In the case of multisensory integration, sound-evoked activity and its associated motor correlate can be dissociated from spiking activity in the primary visual cortex (V1) (Lohuis et al., 2022; Bimbard et al., 2023). A last example, and the one used in the current study, is the case of communication of prediction error (PE) signals. Hierarchical predictive coding theory has been proposed as a general mechanism of processing in the brain (Rao and Ballard, 1999). The communication of prediction error (PE) signals using spikes and local field potentials (LFPs) recorded from subcortical and cortical regions reveal a large-scale hierarchy PE potentials (Parras et al., 2017).

A major question is whether such distributed signals exhibit a high degree of redundancy (i.e. shared information) or a high degree of synergy (i.e. extra information) about their corresponding task variables. Electrophysiological studies have shown that synergy and redundancy have functional relevance (Nigam et al., 2019; Ince et al., 2017; Park et al., 2018; Giordano et al., 2017; Luppi et al., 2022; Varley et al., 2023). For instance, laminar recordings in V1 suggest that synergistic interactions can efficiently decode visual stimuli better than redundant interactions, even in the presence of noise and over-

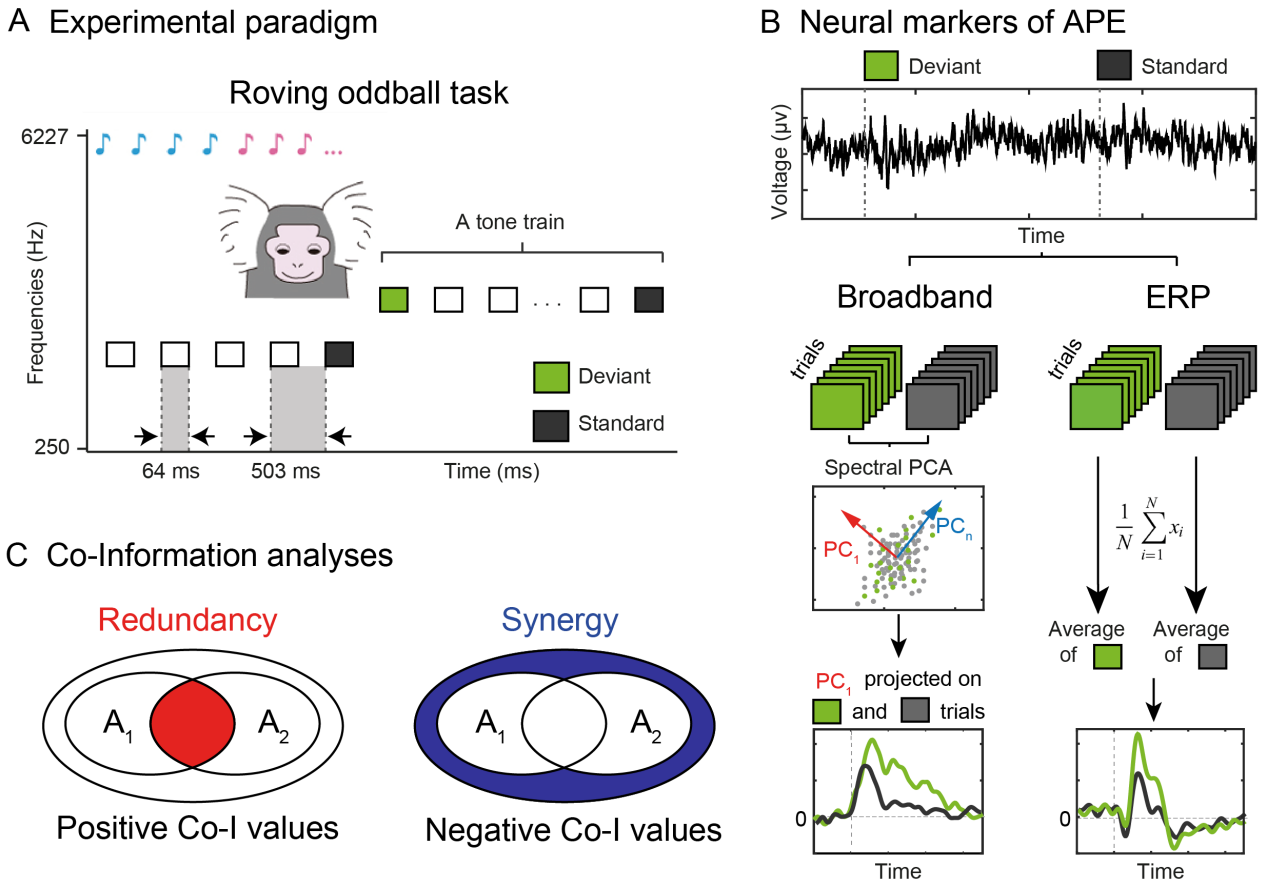

Figure 1: Experimental design, neural markers of PE, and redundancy and synergy analyses **(A)** Using a roving oddball paradigm, 20 different single tones were presented in the trains of 3, 5, or 11 identical stimuli. Any two subsequent trains consisted of different tones. This way, while the adjacent standard (depicted in black) and deviant (depicted in green) tones deviated in frequency due to the transition between the trains, the two expectancy conditions were physically matched, as the first and the last tones of the same train were treated as deviant and standard tones in the analysis of the adjacent stimuli pairs. **(B)** Neural markers of auditory prediction error. Deviant (green) and standard (black) epochs are used to compute the broadband and ERP responses. Broadband is computed by extracting by reconstructing the time series of standard and deviants with the first spectral principal component (SPCA) of the ECoG signal; ERPs are computed by averaging the raw voltage values for standard and deviant trials (see Methods). **(C)** Schematic representation of redundancy and synergy analyses computed using co-Information. Each inner oval (A1 and A2) represents the mutual information between the corresponding ECoG signals and the stimuli category (standard or deviant). The overlap between A1 and A2 represents the redundant information about the stimuli (red; left panel). The outer circle around A1 and A2 represents the the synergistic information about the stimuli (blue; right panel).

lapping receptive fields (Nigam et al., 2019). In contrast, the information processing of olfactory stimuli exhibits higher levels of redundant information across olfactory regions (Olivares et al., 2022). Here we investigate this question by using co-Information (co-I), an information theoretical metric capable of decomposing neural signals into what is informationally redundant and what is informationally synergistic between stimuli (Ince et al., 2017). Redundant information quantifies the shared information between signals, suggesting a common processing of the stimuli. Synergistic information quantifies something different: whether there is extra information only available when signals are combined, indicating that the information about the variable is in the actual relationship between the signals. We analyzed ECoG recordings to investigate spatiotemporal synergy and redundancy in three common marmosets performing an auditory oddball task, which allowed us to determine the processing of communication of prediction error information across the brain

RESULTS

Mutual Information reveals prediction error effects within cortical areas

First, we quantified PE within cortical areas by contrasting deviant and standard tones in each of the three marmosets. For each electrode, we used Mutual Information (MI) to quantify the relationship between tone type on each trial (standard vs deviant) and the corresponding ECoG signal.

Within the framework of information theory, MI is a statistical quantity that measures the strength of the dependence (linear or non-linear) between two random variables. It can be also seen as the effect size, quantified in bits, for a statistical test of independence (Ince et al., 2017). Thus, for each electrode and time point, we considered ECoG signals corresponding to standard and deviant trials and utilized MI to quantify the effect size of their difference.

Cortical mechanisms of auditory prediction error (PE)

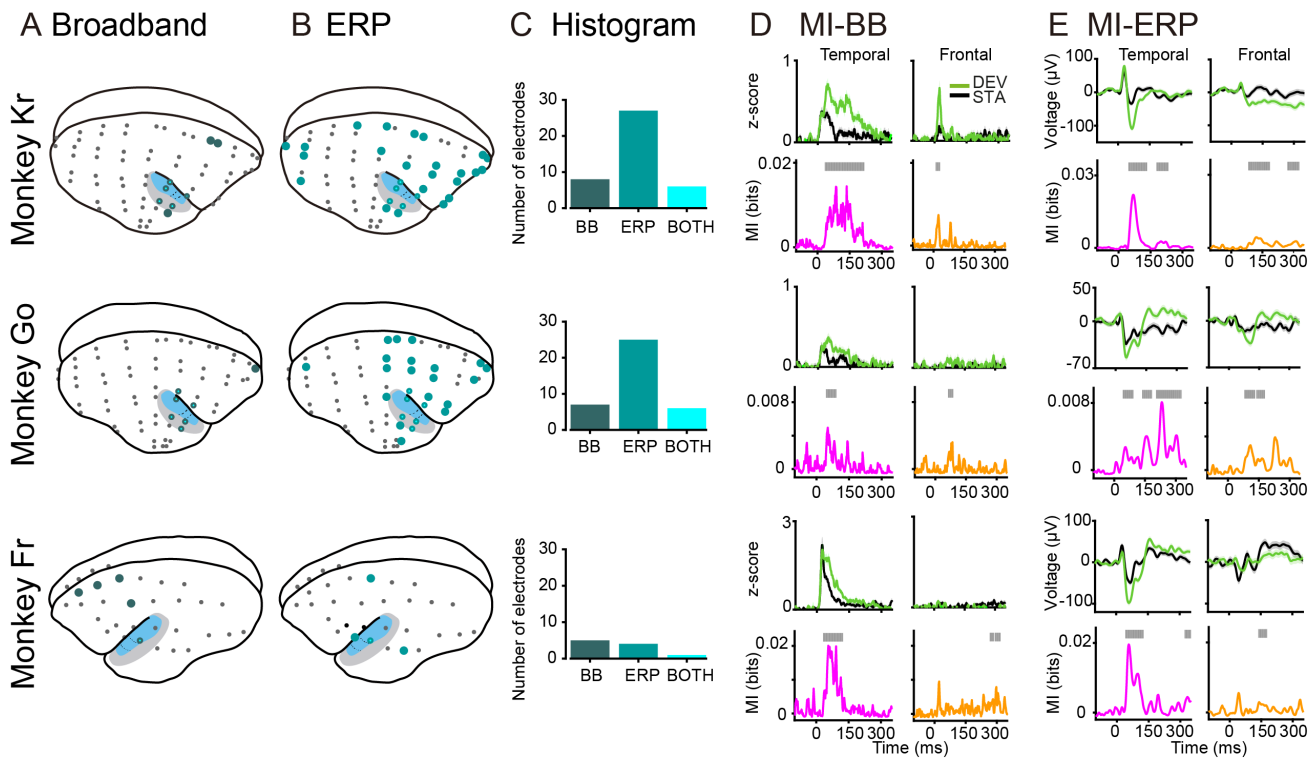

Figure 2: Broadband and ERP markers of PE across the monkey brain. Electrode locations for marmoset Kr (64 electrodes; upper panel), Go (64 electrodes; middle panel), and Fr (32 electrodes; lower panel). Electrodes showing significant PE effect after computing MI between standard and deviant trials for the **(A)** Broadband (dark green circles) and **(B)** ERP (light green circles) markers of auditory prediction error in the three monkeys. Electrodes showing significant MI for both markers are depicted in cyan. **(C)** Histogram of electrodes showing significant MI between tones for BB (left), ERP (middle), and both markers (right) for each animal. **(D)** Electrodes with the highest MI in the temporal and frontal cortex showing the BB signal for deviant and standard tones. Deviant tone (green) and standard tone (black), and the corresponding MI values in bits (effect size of the difference) for the temporal (pink trace) and frontal (orange trace) electrodes. Significant time points after a permutation test are shown as grey bars over the MI plots. **(E)** Electrodes with the highest MI in the temporal and frontal cortex showing the ERP signal for deviant and standard tones. Color codes are the same as in **C**.

have been extensively studied using evoked-related potentials (ERP) and spectral analyses (Canales-Johnson et al., 2021; Blenkmann et al., 2019; Chao et al., 2018; Jiang et al., 2022; Parras et al., 2017). A well-studied ERP marker of auditory PE is the mismatch negativity (MMN), an event-related potential (ERP) that peaks around 150–250 ms after the onset of an infrequent acoustic stimulus (Parras et al., 2017). A second neural marker of auditory PE is the broadband response (BB) (Canales-Johnson et al., 2021). Whereas ERPs reflect a mixture of local potentials and volume conducted potentials from distant sites, BB is an electrophysiological marker of underlying averaged spiking activity generated by the thousands of neurons that are in the immediate vicinity of the recording electrodes (Miller, 2019; Lachaux et al., 2012). MI was computed separately for the two neural markers of prediction error (i.e. ERP and BB signals). Electrodes showing significant differences in MI over time (see i) are depicted in Figure 2. The ERP signal showed PE effects across multiple cortical regions not necessarily restricted to canonical auditory areas (Figure 2B). In the case of the BB signal, MI analyses revealed PE effects located predominantly in the auditory cortex of the three marmosets, as well as in a few electrodes located in the frontal cortex of marmoset Kr and Go (Figure 2A). These results agree with previous studies in different sensory modalities (Miller, 2019) showing that broadband responses are spatially localized.

Co-Information reveals redundant and synergistic interactions within cortical areas

To investigate how auditory PE signals are integrated within and between the cortical hierarchy, we quantified redundant and synergistic cortical interactions using an information theoretical metric known as co-Information (co-I) (Ince et al., 2017). Critically, co-I unravels the specific type of information relationship between signals: positive co-I indicates redundant interactions between signals; and negative co-I accounts for synergistic interactions (Figure 1C). Redundancy implies that the signals convey the same information about PE, indicating a shared encoding of PE information across time or space from trial to trial. On the other hand, synergy implies that signals from different time points or areas convey extra information about PE only when considered together, indicating that the relationship itself contains information about PE that is not available from either of the signals alone (Figure 1C).

To quantify the dynamics of redundancy and synergy temporally and spatially (see i), we computed the co-I within and between cortical areas. We analyzed ERP and BB markers of PE

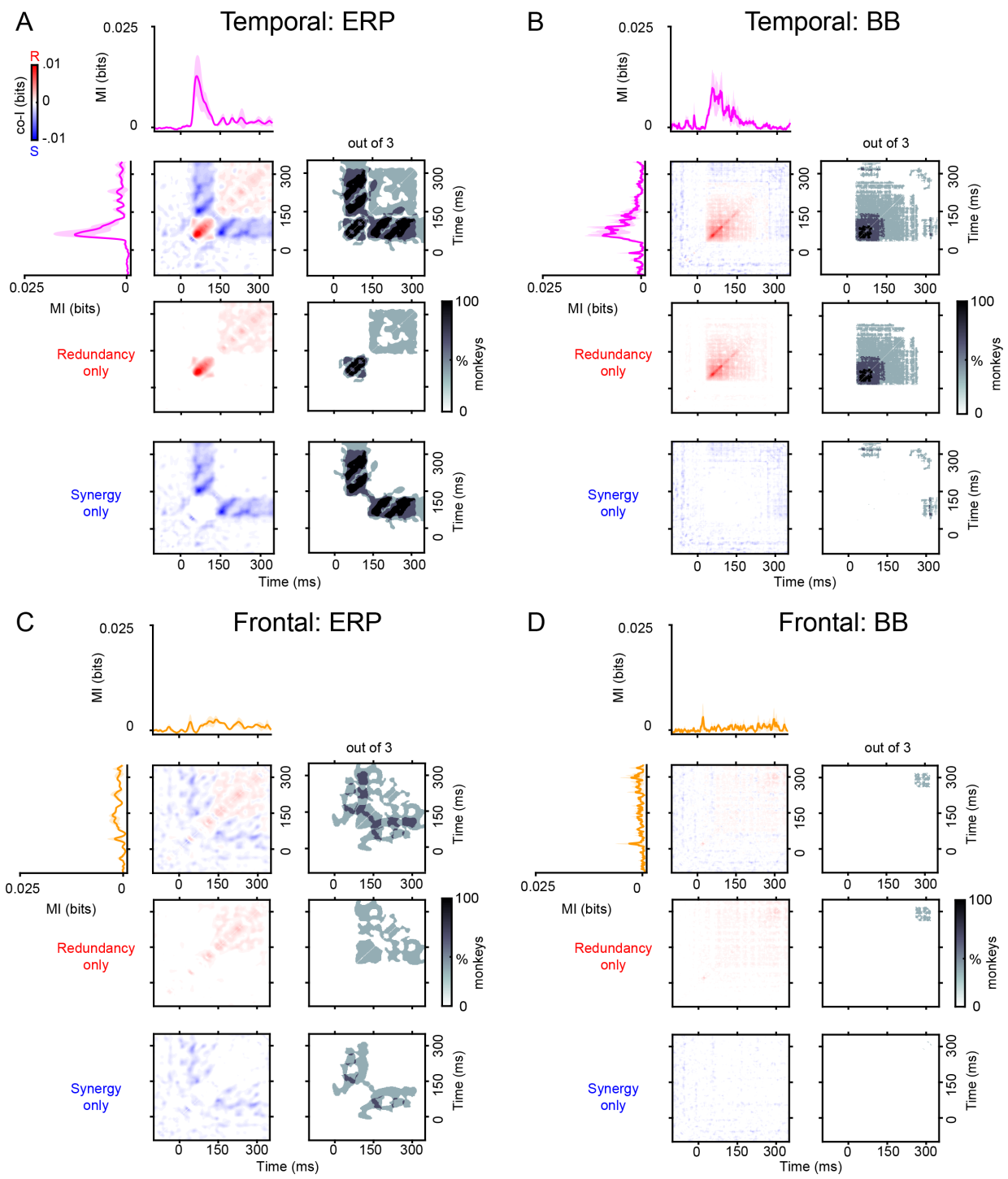

Figure 3: Temporal synergy and redundancy within ERP and BB signals in auditory and frontal electrodes. Co-information revealed synergistic and redundant temporal patterns within ERP (**A**) and BB (**B**) signals in the auditory cortex, and within ERP (**C**) and BB (**D**) signals in the frontal cortex. MI (solid traces) between standard and deviant trials for auditory (pink color) and frontal (orange color) electrodes averaged across the three monkeys. Temporal co-I was computed within the corresponding signal (ERP, BB) across time points between -100 to 350 ms after tone presentation. The average of the corresponding electrodes across monkeys is shown for the complete co-I chart (red and blue panel); for positive co-I values (redundancy only; red panel); and for negative co-I values (synergy only; blue panel). The grey panels show the proportion of monkeys showing significant co-I differences in the single electrodes analysis depicted in Figure S1.

separately, focusing our contrasts on the electrodes that showed significant MI effects in the analyses described in Figure 2.

Temporal synergy and redundancy

We first characterized synergistic and redundant temporal interactions within ERP signal and BB signals (Figure 3 and Figure S1). Co-I analyses revealed widespread temporal clusters

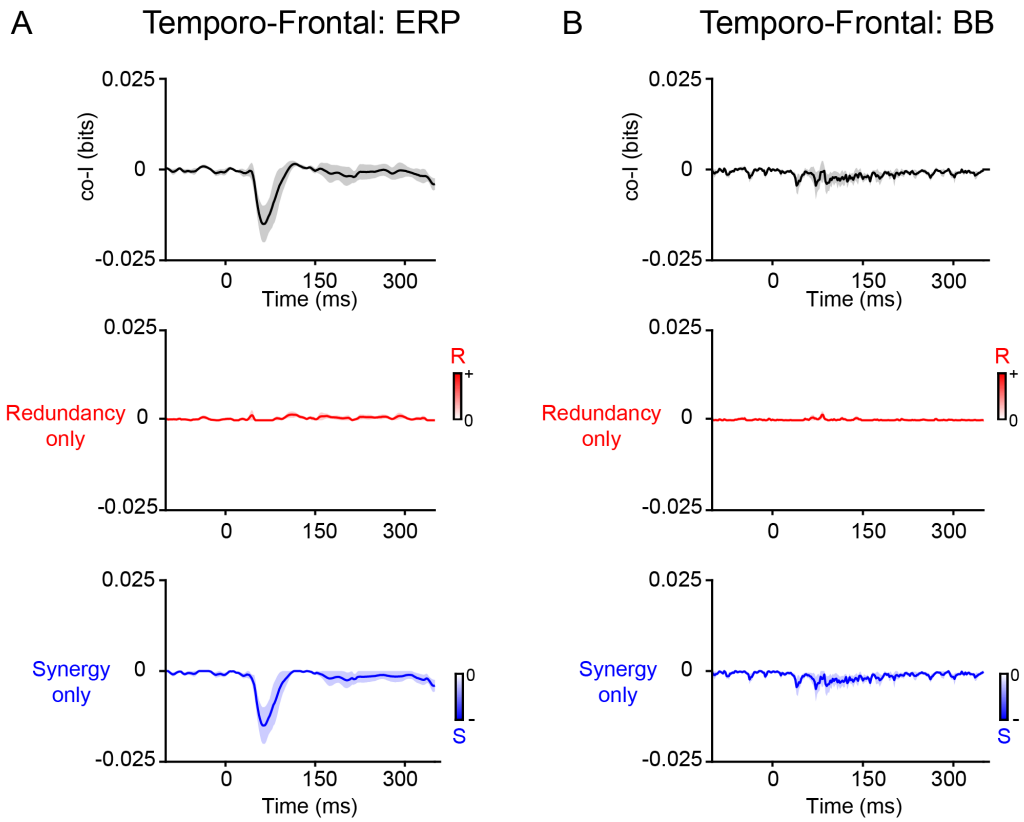

Figure 4: Spatial synergy and redundancy between auditory and frontal electrodes. **A**) Co-Information between auditory and temporal electrodes in the ERP signal. **B**) Co-Information between auditory and temporal electrodes in the BB signal. Significant spatial synergy was observed in the ERP signal between temporo-frontal electrodes. The average of the corresponding temporo-frontal pairs across the three monkeys is shown for the complete co-I values (grey trace), for positive co-I values (redundancy only; red panel), and for negative co-I values (synergy only; blue panel).

of synergistic information (in blue) and redundant information (in red) across the three monkeys in the auditory cortex (Figure 3A,B), and frontal cortex (Figure 3B,D). In the case of the ERP signal, the auditory (Figure 3A,C) and frontal (Figure 3A,B) electrodes showed characteristic off-diagonal synergistic patterns, resulting from the interaction between early and late time points within the same ERP signal. This effect was consistent in the three marmosets (Figure 3A,C; grey clusters between ~140-300 ms after tone presentation), and revealed by the single electrode contrast depicted in Figure S1.

We observed significant temporal redundancy in the auditory (Figure 3B) and frontal (Figure 3D) BB signals. For auditory BB signals, the dynamics of the redundant patterns were observed along the diagonal of the co-Information chart, they were sustained over time and observed between time points around the early MI peaks (i.e., during the transient period when the effect sizes are larger between tones) (Figure 3B; grey clusters ~120-280 ms after one presentation). In the frontal electrodes, we observed significant clusters of sustained redundant interactions around later time points (Figure 3D; grey cluster around 300 ms after tone presentation).

Spatial synergy and redundancy

We next characterized the redundancy and synergy between auditory and frontal electrodes (Figure 4). To this end, we computed the co-I between auditory and frontal pairs of electrodes for the same time points between signals (i.e. not across time points) to emphasize the spatial dimension of the inter-areal interactions. Spatial co-I was computed between the auditory and frontal electrodes used for the temporal co-I (Figure 4) and averaged across monkeys separately for the ERP and BB signals. The results showed that only ERP signals convey spatial information about PE between areas (Synergistic peak ~50-70 ms after tone presentation).

Spatio-temporal synergy and redundancy

We finally characterized spatio-temporal synergistic and redundant interactions across auditory and frontal electrodes (Figure 5 and Figures S2, S3). In the case of the ERP signals, the dynamics of the synergistic interactions was more heterogeneous, showing effects along the diagonal of the co-information chart (Figure 5A; blue clusters along the diagonal ~0-350 ms after tone presentation), but also exhibiting off-diagonal patterns between early time points of the auditory electrodes and later time points in the frontal electrodes (Figure 5A; blue clusters between ~120-350 ms after tone presentation).

In the case of the BB signals, the dynamics of the synergistic interactions were observed off-diagonally in the co-information chart (Figure 5B; blue cluster between 150 ms and 350 ms after tone presentation). On the other hand, redundancy was ob-

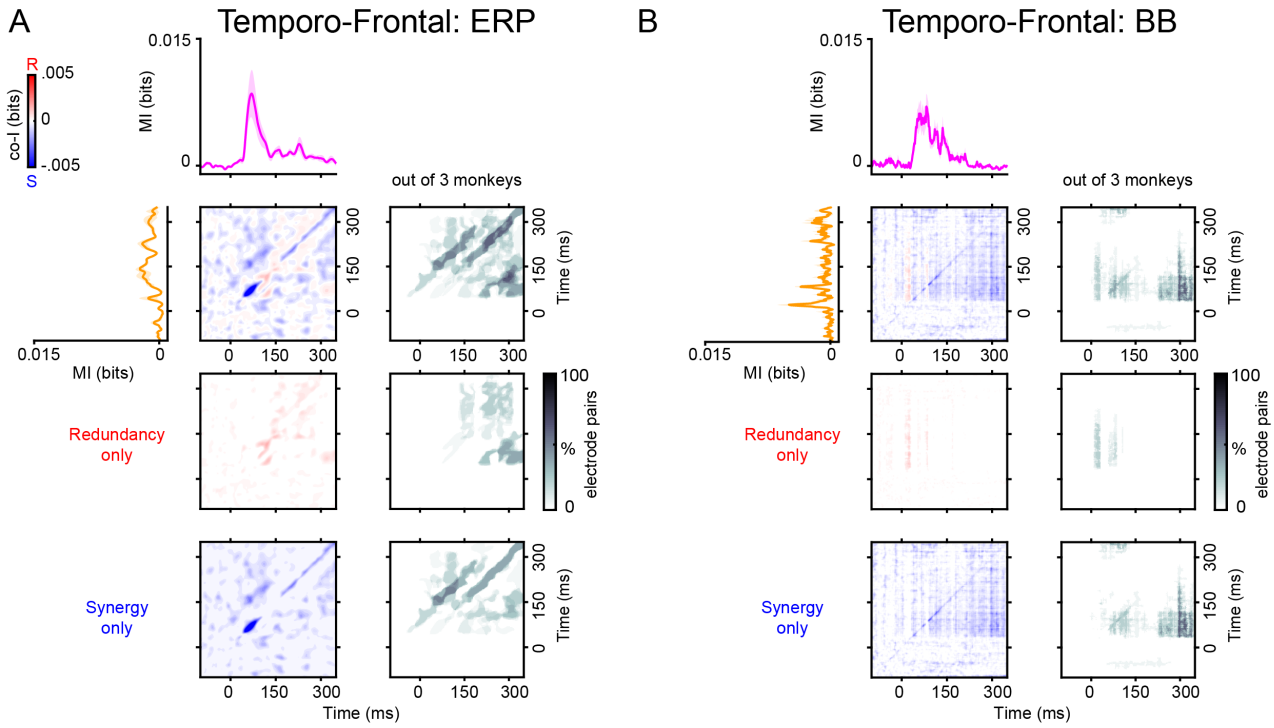

Figure 5: Spatio-temporal synergy and redundancy between auditory and frontal electrodes. Co-information revealed synergistic and redundant spatio-temporal patterns between auditory and frontal electrodes in the ERP (**A**) and BB (**B**) signals. MI (solid traces) between standard and deviant trials for temporal (pink color) and frontal (orange color) electrodes. Co-I was computed between each pair of electrodes and across time points between -100 to 350 ms after tone presentation. The average of the temporo-frontal pairs across the three monkeys is shown for the complete co-I chart (red and blue panel); for the positive co-I values (redundancy only; red panel); and for the negative co-I values (synergy only; blue panel). The proportion of electrode pairs showing significant co-I differences is shown in the corresponding grey panels. The average co-I charts for the individual monkeys are shown in Figures S2 for the ERP signal, and in Figure S3 for the BB signal.

served around time points with maximal MI between auditory and frontal electrodes (Figure 5B; red cluster ~50-70 ms after tone presentation).

To sum up, we observed widespread patterns of synergy within and between electrodes in the temporal and frontal cortices. The dynamics of the synergistic information were observed across distant time points between cortical regions, usually between early and late time points after stimuli presentation. These results suggest that PE information is integrated between areas at both low and high levels of the cortical hierarchy in a synergistic manner, encoded both in time and space by ERP and BB signals.

DISCUSSION

Interpreting redundant interactions

In this study, we focused on computing temporally-resolved metrics of redundancy and synergy, aiming at investigating the dynamics of the information interdependencies within and between cortical signals. Due to the interplay between temporal and spatial information about prediction error, our dynamical approach revealed a rich repertoire of redundant and synergistic patterns, showing transient and sustained information dynamics. Thus, we showed that information was redundant or synergistic across specific time windows, and emerged within or between brain areas.

Redundant patterns of information were observed mainly at time points close to the diagonal of the co-I chart, both within signals (Figure 3) and between signals (Figure 5). The advantage of computing redundancy is that it reveals to which extent local and inter-areal signals represent the same information about the stimuli category on a trial-by-trial basis. Redundant interactions about tone category (i.e., deviant or standard) were observed in the ERP and BB signals and represented the outcome of the shared information acrross time points (temporal redundancy) and between areas (spatio-temporal redundancy). These observed redundancy patterns raise the question of what is the functional relevance of redundant information for processing PE across the cortex.

A neurobiological interpretation of redundancy is that the neural populations encoding this type of information share a common mechanism (Ince et al., 2017). From the perspective of cortical dynamics, redundancy then could provide cortical interactions with robustness (Luppi et al., 2022; Olivares et al., 2022), as redundant interdependencies convey information that is not exclusive to any single cortical region. Robustness, understood as the ability to tolerate perturbations that might affect network functionality (Luppi et al., 2022), is a desirable characteristic of cortical networks processing predictions to preserve stimuli separability in the presence of highly variable stimuli features, environmental noise, or endogenous sources of noise such as background neural activity. Thus, our results suggest

that redundancy quantifies the robustness of the information processing in the cortex, enabling multiple areas to process common information about prediction errors.

Interpreting synergistic interactions

A different type of dynamics was observed in the case of the synergistic information across the cortex. While redundant information was observed near the diagonal of the co-I charts, synergistic information was observed mainly off-diagonally, i.e. between early and late times points after tone presentation (Figure 3). This indicates that late temporal responses carry information that, in combination with the early one, provides extra information about the identity of the tone (standard or deviant) than when considered in isolation. A neurobiological interpretation of synergy is that the underlying neural populations encode independent but complementary information (Ince et al., 2017).

This raises the question about what is the functional relevance of synergistic information for representing prediction errors. We propose that synergistic interactions could represent a neural marker of biological degeneracy. Degeneracy is the ability of structurally different elements to perform the same function, being a ubiquitous property of many biological systems including neural circuits and networks (Edelman and Gally, 2001). Importantly, degenerative systems are capable of performing different functions (i.e., generalizability and pluripotency) when exposed to changes in contextual circumstances, making them extremely flexible and resilient (Edelman and Gally, 2001).

There is evidence that degeneracy in neural networks may provide various computational benefits, for example, enabling stable computations despite unstable neural dynamics (Driscoll et al., 2017; Druckmann and Chklovskii, 2012) and allowing the central nervous system to filter out unwanted noise (Moreno-Bote et al., 2014). The cortical markers of auditory PE have been observed in auditory subcortical and cortical structures of several species despite the differences in their neuroanatomical structures (Parras et al., 2017; Blenkmann et al., 2019; Canales-Johnson et al., 2021). This suggests that synergistic information is the outcome of distinct neural circuits computing error information in a complementary manner, providing the cortex with a flexible code for representing PE information distributively.

Implications for predictive coding theories

Here we investigated a relevant but relatively unexplored aspect of inter-areal interactions: their information content. Traditionally, inter-areal interactions in predictive processing are studied with metrics derived from spectral decomposition such as coherence or Granger-causality (GC) (Vinck et al., 2022). Although useful, a limitation of these metrics (directional or not) is that they can only quantify the amount of coupling between signals rather than their information content. Thus, even in cases where these metrics account for inter-areal differences between stimuli or task variables, it is unclear whether the information carried by the interactions is the same or not on a trial-by-trial basis. For example, consider the case where GC distinguishes standard and deviant tones between fronto-temporal regions (Chao et al., 2018). Is the information conveyed by these interactions the same (redundant) or complementary (synergistic)?

To answer this question we need tools that quantify the type of information carried by these interactions rather than just their degree of coupling. Thus, in this study, we moved away from traditional metrics of inter-areal interactions in predictive processing (Vinck et al., 2022), and we investigated distributed patterns of information using metrics of redundancy and synergy. This notion can have ramifications for predictive processing accounts. For example, the finding that synergistic information about PE can emerge within signals in the initial stages of the auditory hierarchy (A1) suggests a more distributed form of computation than postulated by Hierarchical Predictive Coding (HPC) (Chao et al., 2018; Jiang et al., 2022). HPC postulates that PE information should be integrated into successive stages of the hierarchy, from sensory areas (A1) to higher-order areas (frontal cortex). This processing sequence is accompanied by gradual increases in the spatiotemporal processing and complexity of stimuli features. Our findings suggest the alternative view, in line with a more distributed view of brain processing (Steinmetz et al., 2019; Parras et al., 2017; Voitov and Mrsic-Flogel, 2022). Rather than a hierarchy of prediction error processing, we propose that PE information can be encoded in parallel across different temporal and spatial scales.

Authorship contributions

Conceptualization: ACJ, RI, and MV. Data analysis: FG and ACJ. Marmoset recordings and surgeries: MK. Software and methods for marmoset data: RI, MJ, and KM. Writing and editing: ACJ, CU, and MV. Supervision: ACJ.

METHODS

Data acquisition

The dataset the current study used consists of ECoG recordings of implanted electrodes in three adult male common marmosets (*Callithrix jacchus*). The details of the complete dataset have been described previously (Canales-Johnson et al., 2021; Komatsu et al., 2015).

The ECoG recordings were acquired in a passive listening condition while the monkeys were awake. During the recording sessions, the monkeys Go and Kr sat on a primate chair in a dimly lit room, while monkey Fr was held in a drawstring pouch, which was stabilized in a dark room. Every session lasted for about 15 minutes of which the first 3 minutes of data were used for various standard stimuli and the remaining 12 minutes of data acquisition were dedicated to the roving oddball sequences. For the data analysis, we acquired a total of three sessions for monkey Fr, which resulted in 720 (240 × 3) standard and deviant trials, and six sessions for monkeys Go and Kr, resulting in 1440 (240 × 6) standard and deviant trials. For the recordings, a multi-electrode data acquisition system was used (Cerebus Blackrock Microsystems, Salt Lake City, UT, USA) with a band-pass filter of 0.3–500 Hz and then digitised at 1 kHz. In the signal pre-processing, those signals were re-referenced using an average reference montage, and high-pass filtered above 0.5 Hz, using a 6th order Butterworth filter.

The recording was done with chronically implanted, customized multielectrode ECoG electrode arrays (Cir-Tech Inc., Japan). Before implantation with the ECoG electrode arrays, the monkeys were anaesthetized and further suffering was minimized. Both surgical and experimental procedures were performed in accordance with the National Institutes of Health Guidelines for the Care and Use of Laboratory Animals and approved by the RIKEN Ethical Committee (No. H26-2-202). The locations of the implanted electrodes of each monkey are found in Figure 2. All electrodes were implanted in epidural space; 28 in the left hemisphere and an additional 4 in the frontal cortex of the right hemisphere of monkey Fr, 64 in the right hemisphere of monkey Go, and 64 in the right hemisphere of monkey Kr. In the 32-electrode array, each electrode contact was 1 mm in diameter and had an inter-electrode distance of 2.5 - 5.0 mm (Komatsu et al., 2015). In the 64-electrode array, each electrode contact was 0.6 mm in diameter and had an inter-electrode distance of 1.4 mm in a bipolar pair (Komatsu et al., 2019). The electrode arrays covered the temporal, parietal, frontal, and occipital lobes.

Experiment task

For the experiment, the monkeys were subjected to a roving oddball paradigm (Canales-Johnson et al., 2021). Trains of 3, 5, or 11 repetitive single-tones of twenty different frequencies (250-6727 Hz with intervals of 1/4 octave) were presented in a pseudo-random order. Within each tone train the presented tones had the same frequency, but between tone trains the frequency was different. As the tone trains followed each other continuously, the first tone of a train was considered an unexpected deviant tone, because the preceding tones were of a different frequency, while the expected standard tone was defined as the final tone in a train because the preceding tones were of the same frequency (Figure 1A). The presented tones were pure sinusoidal tones that lasted for 64 ms (7 ms rise/fall) and the time between stimulus onsets was 503 ms. Stimulus presentation was controlled by MATLAB (MathWorks Inc., Natick, MA, USA) using the Psychophysics Toolbox extensions (Brainard and Vision, 1997). Two audio speakers (Fostex, Japan) were used to present the tones with an average intensity of 60 dB SPL around the animal's ear.

ERP and BB analyses

For further analysis, the raw ECoG voltage responses have been transformed into ERP and BB as described in Canales-Johnson et al. (2021). In brief, common average referencing was used to re-reference the ECoG recordings across all electrodes. For obtaining ERPs, a low-pass filter of 1-40 Hz was applied for the ERP analysis. Standard and deviant tones were categorized as described before. Epochs of -100 ms to 350 ms around the onset of the tones were taken, and a baseline correction was applied by subtracting the mean voltage during the 100 ms period before the stimulus onset from the total epoch. The MMN signal was determined by subtracting the deviant ERP from the standard ERP. After the initial inspection, the three best electrodes of the temporal region were selected for each monkey (Figure 1B). This was based on the amplitude of the MMN in the ERP.

In order to obtain the BB, spectral decoupling of the raw ECoG was carried out (Canales-Johnson et al., 2021; Miller, 2019). To extract the course of broadband spectral activity, the spectral decoupling of the raw ECoG signal was carried out. As for the ERP analysis, common average referencing was used to re-reference ECoG potentials of all the electrodes. Epochs of -100 ms to 350 ms around the onset of the tones were used to calculate discrete samples of power spectral density (PSD). Trials from both conditions were grouped together and individual PSDs were normalized with an element-wise division by the average power at each frequency, and the obtained values were log-transformed. In order to identify components of stimulus-related changes in the PSD, a principal component method is applied. This consists of calculating the covariance matrix between the frequencies. The eigenvectors of this decomposition are called Principal Spectral Components (PSCs), and reveal distinct components of neural processing, hence enabling us to identify stimulus-related changes in the PSD. Afterward, the time series were z-scored per trial to get intuitive units, then exponentiated and subtracted by 1. Finally, a baseline correction was performed by subtracting the mean value of the pre-stimulus period of -100 to 0 ms.

Both for the ERP and BB signals some electrodes were excluded from further analysis. This was done because the signal was absent or clearly erroneous. Electrode 18 in Fr was excluded from the ERP analysis, while electrodes 18 in Fr, 30, 44, 45 in Go, and 30 in Kr were excluded from the BB analysis.

Mutual Information analyses

In order to quantify the MI between the stimulus class and the ECoG signal (both ERP and BB), the GCMI toolbox (Gaussian Copula Mutual Information) (Ince et al., 2017) was used. This toolbox calculates the MI based on the Gaussian copula the raw ERP or BB data transforms to. The approach combined a permutation test with 1000 permutations together with a method of maximum statistics in order to correct for multiple comparisons. Using all available trials, the signal at every time point was permuted 1000 times for each electrode, randomly assigning the stimulus class labels each time. The maximum value at each time point was taken, and the 95th percentile of this value was used as the threshold for significance. This method corrects for multiple comparisons and provides a Family-Wise Error Rate (FWER) of 0.05.

Co-information analyses

We quantified co-Information (co-I) within signals (single electrodes) and between signals (between pairs of electrodes) using the GCMI toolbox (Ince et al., 2017). The co-I was calculated by comparing signals on trial by trial basis. This resulted in a quantification of the information content, redundant or synergistic, between the two signals. The co-information (co-I) was calculated in the following way:

$$coI(X;Y;S) = I(X;S) + I(Y;S) - I(X,Y;S)$$

For each time point, $I(X;S)$ corresponds to the mutual information (MI) between the signal at recording site X and stimuli class S. $I(Y;S)$ corresponds to the MI between the signal at recording site Y and stimuli class S. Finally, $I(X,Y;S)$ corresponds to the MI between stimuli class S combining signals from recording sites X and Y.

For each neural marker of auditory PE (i.e., ERP and BB), co-information was computed for each pair of tones (standard and deviants) within recordings sites in A1 and frontal regions (Figure 3 and Figure S1), and between A1 and frontal regions (Figure 4, 5 and Figure S1, S2,). Positive co-information shows that signals between recording sites contain redundant, or overlapping, information about the stimuli. Negative co-information corresponds to the synergy between the two variables: the information when considering the two variables jointly is larger than considering the variables separately.

Figure 1C shows a schematic representation of co-I between two signals. It shows the independent information that response 1 and response 2 (both in white) contain. If there is an overlap in the information that is being represented by the two signals, there is a redundancy (red color) in the information that the two responses contain. If the two signals considered together contain more information than could be expected based on the information present in the individual signals, there is synergy (blue color).

Statistical analyses of co-I charts were performed by using a permutation test with 1000 permutations and using the same maximum statistics method described for the MI analyses, resulting in a FWER of 0.05.

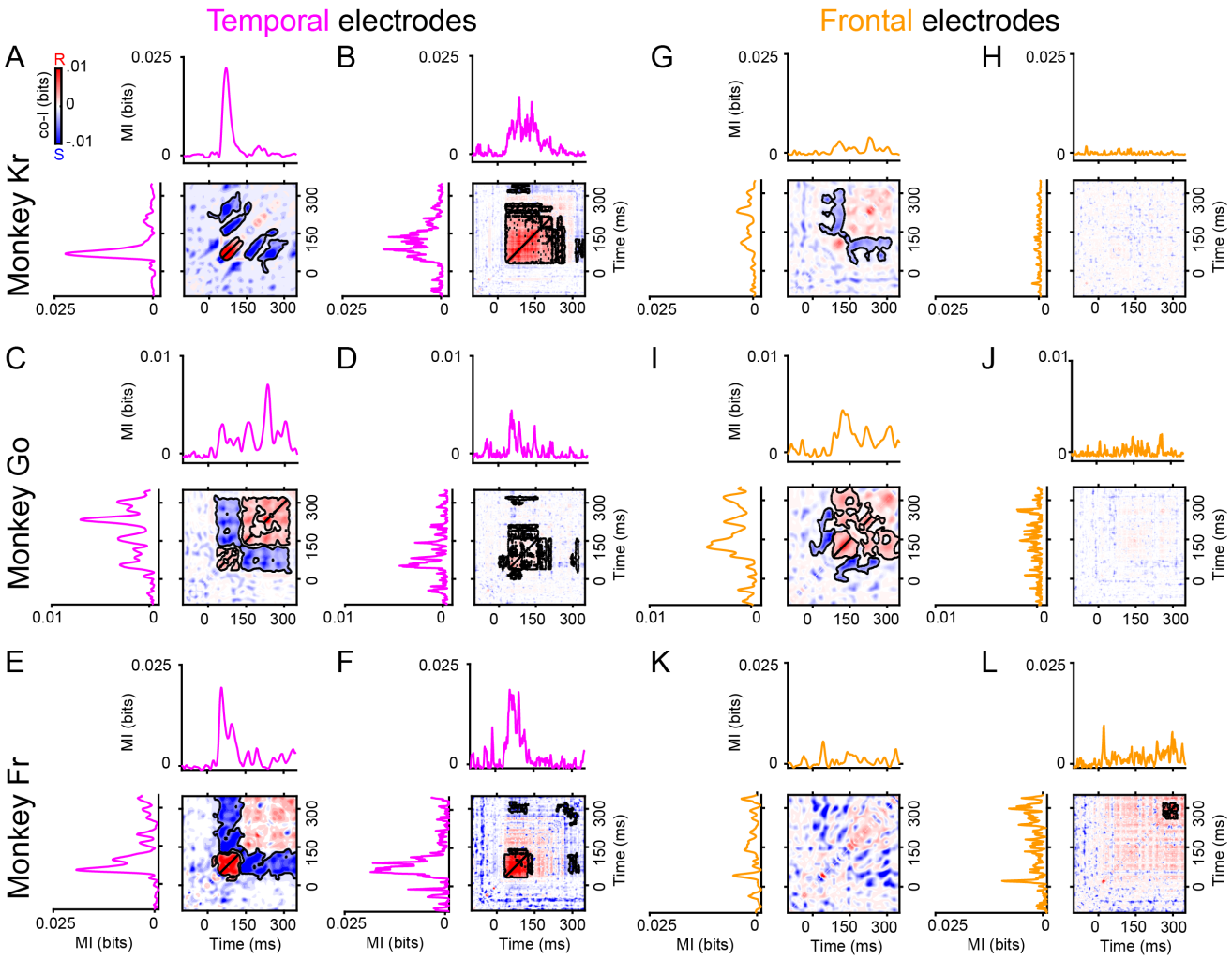

Figure S1: Synergy and redundancy within ERP and within BB signals in temporal and frontal regions Co-information within auditory **(A, C, E)**, and frontal **(G, I, K)** electrodes in the ERP signal. Co-information within auditory **(B, D, F)**, and frontal **(H, J, L)** electrodes in the BB signal. MI (solid traces) between standard and deviant trials for temporal (pink color) and frontal (orange color) electrodes. Co-I was computed between each pair of electrodes and across time points between -100 to 350 ms after tone presentation. Significant temporal clusters after a permutation test (see Methods) are depicted in black contours.

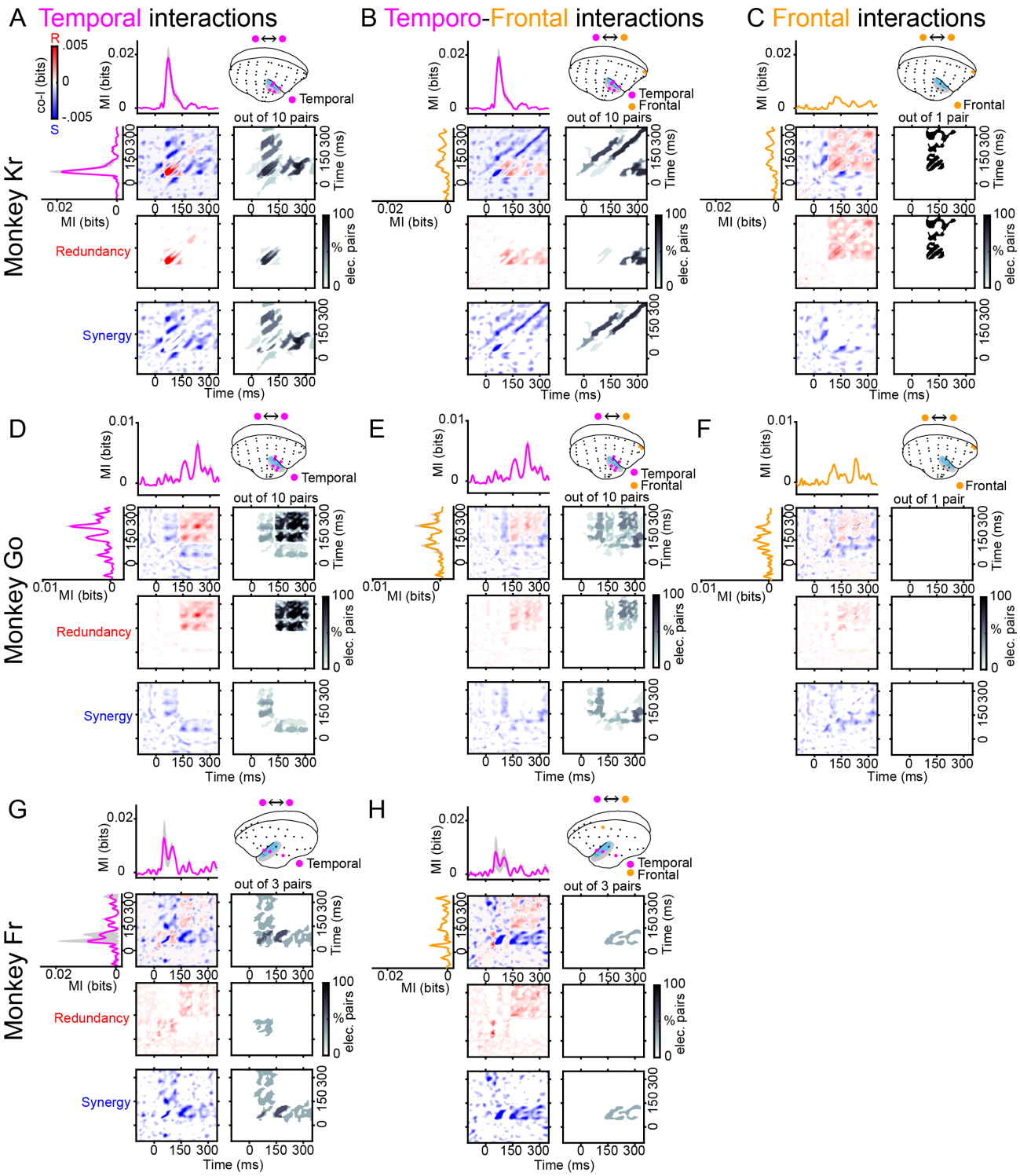

Figure S2: Synergy and redundancy between ERP signals and across cortical areas in the three marmosets. Co-information revealed synergistic and redundant PE patterns across temporal **(A, D, G)**, temporo-frontal **(B, E, H)**, and frontal **(C, F)** electrodes. MI (solid traces) between standard and deviant trials for temporal (pink color) and frontal (orange color) electrodes. Co-I was computed between each pair of electrodes and across time points between -100 to 350 ms after tone presentation. The average of the corresponding electrode pairs per (i.e. temporal, temporo-frontal, and frontal) is shown for the complete co-I values (red and blue panel), for positive co-I values (redundancy only; red panel), and negative co-I values (synergy only; blue panel).

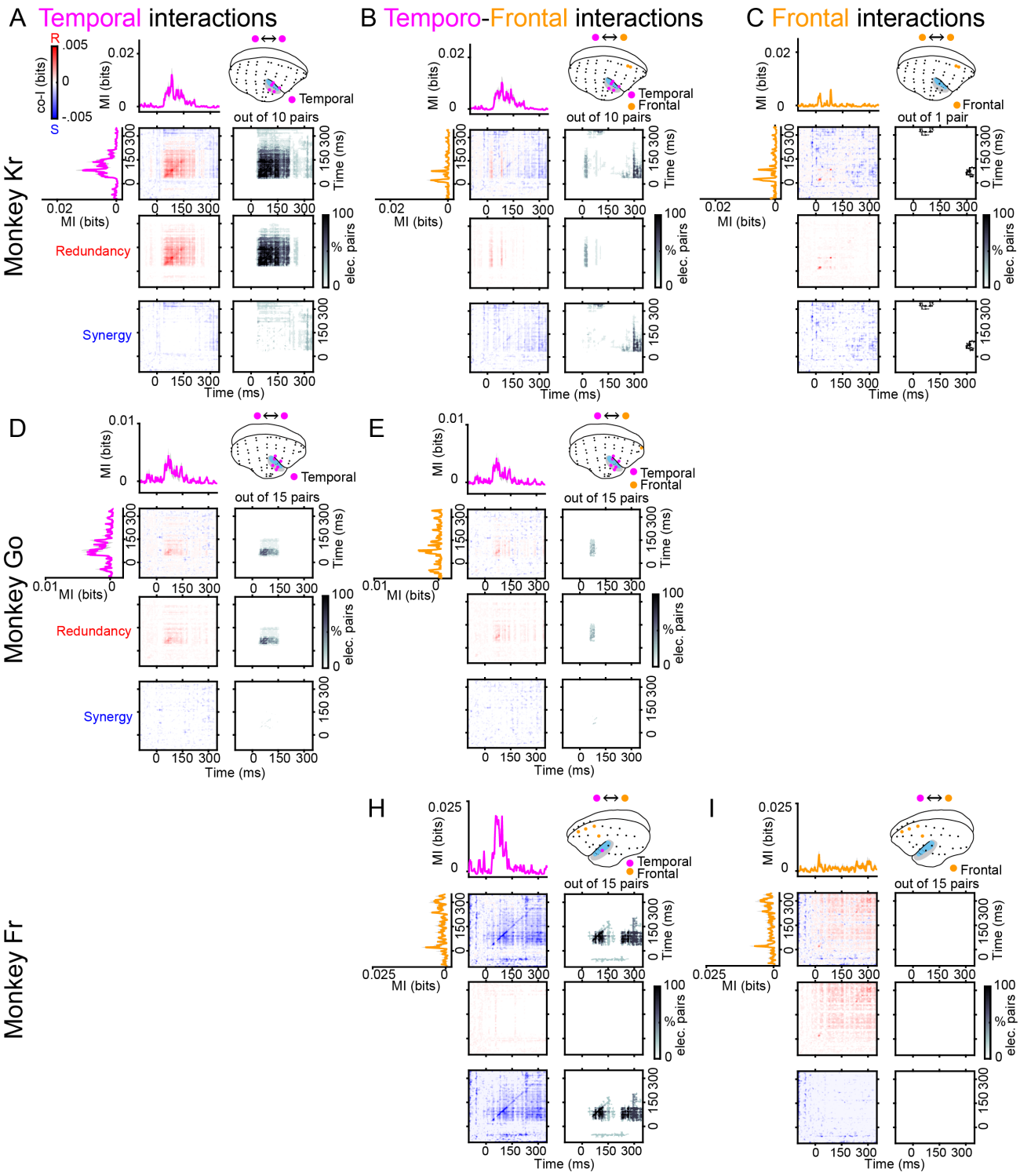

Figure S3: Synergy and redundancy between BB signals and across cortical areas in the three marmosets. Co-information revealed synergistic and redundant PE patterns across temporal **(A, D)**, temporo-frontal **(B, E, H)**, and frontal **(C, I)** electrodes. MI (solid traces) between standard and deviant trials for temporal (pink color) and frontal (orange color) electrodes. Co-I was computed between each pair of electrodes and across time points between -100 to 350 ms after tone presentation. The average of the corresponding electrode pairs per (i.e. temporal, temporo-frontal, and frontal) is shown for the complete co-I values (red and blue panel), for positive co-I values (redundancy only; red panel), and negative co-I values (synergy only; blue panel).

References

Bimbard, C., Sit, T.P.H., Lebedeva, A., Reddy, C.B., Harris, K.D., Carandini, M., 2023. Behavioral origin of sound-evoked activity in mouse visual cortex. Nat. Neurosci. .

Blenkmann, A.O., Collavini, S., Lubell, J., Llorens, A., Funderud, I., Ivanovic, J., Larsson, P.G., Meling, T.R., Bekinschtein, T., Kochen, S., Endestad, T., Knight, R.T., Solbakk, A.K., 2019. Auditory deviance detection in the human insula: An intracranial eeg study. Cortex 121, 189–200.

Breakspear, M., 2017. Dynamic models of large-scale brain activity. Nat. Neurosci. 20, 340–352.

Canales-Johnson, A., Teixeira Borges, A.F., Komatsu, M., Fujii, N., Fahrenfort, J.J., Miller, K.J., Noreika, V., 2021. Broadband dynamics rather than frequency-specific rhythms underlie prediction error in the primate auditory cortex 41, 9374–9391.

Chao, Z.C., Takaura, K., Wang, L., Fujii, N., Dehaene, S., 2018. Large-scale cortical networks for hierarchical prediction and prediction error in the primate brain. Neuron 100, 1252–1266.e3.

Driscoll, L.N., Pettit, N.L., Minderer, M., Chettih, S.N., Harvey, C.D., 2017. Dynamic reorganization of neuronal activity patterns in parietal cortex. Cell 170, 986–999.e16.

Druckmann, S., Chklovskii, D.B., 2012. Neuronal circuits underlying persistent representations despite time varying activity. Curr. Biol. 22, 2095–2103.

Edelman, G.M., Gally, J.A., 2001. Degeneracy and complexity in biological systems. Proc. Natl. Acad. Sci. U. S. A. 98, 13763–13768.

Giordano, B.L., Ince, R.A.A., Gross, J., Schyns, P.G., Panzeri, S., Kayser, C., 2017. Contributions of local speech encoding and functional connectivity to audio-visual speech perception. eLife 6, e24763.

Ince, R.A., Giordano, B.L., Kayser, C., Rousselet, G.A., Gross, J., Schyns, P.G., 2017. A statistical framework for neuroimaging data analysis based on mutual information estimated via a gaussian copula. Human Brain Mapping 38, 1541–1573.

Jiang, Y., Komatsu, M., Chen, Y., Xie, R., Zhang, K., Xia, Y., Gui, P., Liang, Z., Wang, L., 2022. Constructing the hierarchy of predictive auditory sequences in the marmoset brain. eLife 11, e74653.

Komatsu, M., Kaneko, T., Okano, H., Ichinohe, N., 2019. Chronic implantation of whole-cortical electrocorticographic array in the common marmoset. J. Vis. Exp. .

Komatsu, M., Takaura, K., Fujii, N., 2015. Mismatch negativity in common marmosets: Whole-cortical recordings with multi-channel electrocorticograms. Sci. Rep. 5, 15006.

Lachaux, J.P., Axmacher, N., Mormann, F., Halgren, E., Crone, N.E., 2012. High-frequency neural activity and human cognition: Past, present and possible future of intracranial eeg research. Progress in Neurobiology 98, 279–301. High Frequency Oscillations in Cognition and Epilepsy.

Lohuis, M.N.O., Marchesi, P., Olcese, U., Pennartz, C., 2022. Triple dissociation of visual, auditory and motor processing in primary visual cortex. bioRxiv .

Luppi, A.I., Mediano, P.A.M., Rosas, F.E., Holland, N., Fryer, T.D., O'Brien, J.T., Rowe, J.B., Menon, D.K., Bor, D., Stamatakis, E.A., 2022. A synergistic core for human brain evolution and cognition. Nat. Neurosci. 25, 771–782.

Miller, K.J., 2019. A library of human electrocorticographic data and analyses. Nat. Hum. Behav. 3, 1225–1235.

Moreno-Bote, R., Beck, J., Kanitscheider, I., Pitkow, X., Latham, P., Pouget, A., 2014. Information-limiting correlations. Nat. Neurosci. 17, 1410–1417.

Nigam, S., Pojoga, S., Dragoi, V., 2019. Synergistic coding of visual information in columnar networks. Neuron 104, 402–411.e4.

Olivares, J., Orio, P., Sadílek, V., Schmachtenberg, O., Canales-Johnson, A., 2022. Neural oscillations across olfactory regions encode odorant information in the teleost olfactory system doi:10.1101/2022.04.15.488302.

Panzeri, S., Moroni, M., Safaai, H., Harvey, C.D., 2022. The structures and functions of correlations in neural population codes. Nat. Rev. Neurosci. 23, 551–567.

Park, H., Ince, R.A.A., Schyns, P.G., Thut, G., Gross, J., 2018. Representational interactions during audiovisual speech entrainment: Redundancy in left posterior superior temporal gyrus and synergy in left motor cortex. PLOS Biology 16, 1–26.

Parras, G.G., Nieto-Diego, J., Carbajal, G.V., Valdés-Baizabal, C., Escera, C., Malmierca, M.S., 2017. Neurons along the auditory pathway exhibit a hierarchical organization of prediction error. Nat. Commun. 8, 2148.

Rao, R.P., Ballard, D.H., 1999. Predictive coding in the visual cortex: a functional interpretation of some extra-classical receptive-field effects. Nat. Neurosci. 2, 79–87.

Saleem, A.B., Diamanti, E.M., Fournier, J., Harris, K.D., Carandini, M., 2018. Coherent encoding of subjective spatial position in visual cortex and hippocampus. Nature 562, 124–127.

de Schotten, M.T., Forkel, S.J., 2022. The emergent properties of the connected brain. Science 378, 505–510.

Shenoy, K.V., Kao, J.C., 2021. Measurement, manipulation and modeling of brain-wide neural population dynamics. Nat. Commun. 12, 633.

Steinmetz, N.A., Zatka-Haas, P., Carandini, M., Harris, K.D., 2019. Distributed coding of choice, action and engagement across the mouse brain. Nature 576, 266–273.

Urai, A.E., Doiron, B., Leifer, A.M., Churchland, A.K., 2022. Large-scale neural recordings call for new insights to link brain and behavior. Nat. Neurosci. 25, 11–19.

Varley, T.F., Sporns, O., Schaffelhofer, S., Scherberger, H., Dann, B., 2023. Information-processing dynamics in neural networks of macaque cerebral cortex reflect cognitive state and behavior. Proc. Natl. Acad. Sci. U. S. A. 120, e2207677120.

Vinck, M., Uran, C., Canales-Johnson, A., 2022. The neural dynamics of feedforward and feedback interactions in predictive processing. doi:10.31234/osf.io/n3afb.

Voitov, I., Mrsic-Flogel, T.D., 2022. Cortical feedback loops bind distributed representations of working memory. Nature 608, 381–389.